Title: SBIS, a new orange fluorescent vital probe for the 4D imaging of brown algal cells

Authors: Marie Zilliox[1], Mayeul Collot[2*], Bénédicte Charrier[1*]

Affiliation:

[1]: Morphogenesis of Brown Algae, UMR5242, Institute of Functional Genomics of Lyon (IGFL), UMR 5242, CNRS, ENS de Lyon, 32-34 avenue Tony Garnier, 69007 Lyon, France

[2]. Chemistry of Photoresponsive Systems, Laboratoire de Chémo-Biologie Synthétique et Thérapeutique (CBST) UMR 7199, CNRS, Université de Strasbourg, F-67400 Illkirch, France

* Corresponding authors:

mayeul.collot@unistra.fr

benedicte.charrier@cnrs.fr

Keywords

brown algae, plasma membrane probes, live cell imaging, cell growth, cell shape, confocal microscopy, 3D microscopy, light-sheet microscopy, seaweeds, *Ectocarpus*, *Sphacelaria*, *Saccharina*

Abstract

Living cells of brown algae are difficult to observe in 3D due to the presence of pigments such as fucoxanthin and chlorophyll that diffract light. Furthermore, they grow slowly in seawater. To gain insight into the shape and size of brown alga cells in 3D during the development of these multicellular photosynthetic organisms, we designed a fluorescence probe that efficiently and selectively labels the plasma membrane. Styryl benzoIndoleninium sulfonate (SBIS) is a bright orange fluorogenic probe that is soluble and virtually non-emissive in seawater; it accumulates in the plasma membrane of brown algal cells, where it activates upon binding. SBIS enabled the 3D observation of cells of different shapes and sizes in several brown alga species, over a period of up to seven days and in a medium mimicking natural growth conditions. More importantly, SBIS makes it possible to observe cells at thicknesses of up to 20 µm, in contrast to Calcofluor White. These properties resulted in the visualization of the entire contour of the cells in the Z-axis of uniseriate filaments of *Ectocarpus,* polystichous filaments of *Sphacelaria* and cellular

monolayered lamina of *Saccharina*. Altogether, SBIS now makes the study of embryogenesis and early development possible in 4D in these brown algae.

Introduction

Brown algae are multicellular marine organisms whose biology is still relatively unexplored. Nonetheless, they can be found along almost all of the planet's coasts, where they contribute to local ecology in a number of ways [1–9]. Brown algae come in various sizes and shapes [3], ranging from long-bladed kelps measuring over 30 m in length to the microscopic filaments of Ectocarpales species. At first glance, their bodies are made up of a mass of cells of fairly uniform shape and color, and seem poorly differentiated [3,10]. However, looking more closely reveals that their shapes change as they mature: the cuboid epidermal cells of the meristoderm of *Saccharina* (Laminariales) differentiate into spherical and cylindrical cortical cells [11]; the oblong apical and cylindrical subapical cells in the filamentous alga *Ectocarpus* differentiate into spherical cells in the center in the filament [12–14]. Even more impressive is the differentiation of the spherical cortical cells into highly branched medullary cells in kelps [11,15]. In all these cases, cell shape change is accompanied by a thickening of the cell wall and a change in metabolic function: kelp meristoderm cells are highly dividing cells whereas medullary cells transport metabolites throughout the organism; the apical cell of the filamentous brown alga *Ectocarpus* is primarily dedicated to tip growth and the round, more mature cells in the center of the filament are more active in photosynthesis [13]. Therefore, brown algae have several cell types with different physiological and metabolic functions, and also feature different cell growth rates and shapes. Progress in the understanding of brown algal biology, and especially development, requires imaging these cells in 3D over time.

Brown algal cells are surrounded by a cell wall (CW), which prevents them from moving within the tissue and gives them a specific shape. Because brown algae are not genetically transformable, it is not possible to visualize cell contours using a fluorescent tag encoded in the genome and expressed throughout the development of the organism. Therefore, a fluorescent vital probe harboring chemical characteristics compatible with the biological features of brown algae must be used. The probe must be suitable for use in seawater, and be stable over several days, because brown algae grow slowly (the *Ectocapus* filament grows 300 times slower than the pollen tube of tobacco [16]). However, by far the most important criterion is the ability of the probe to image brown algal cells in 3D, despite the presence of pigments [17]. Carotenoid pigments are abundant in the chloroplasts of brown algal cells (from 26 to 60%) where they absorb blue light (excitation wavelength, 452 nm) and emit red light (emission wavelength, 655 nm; [18]. In this context, Calcofluor White (CFW) efficiently labels the CW [13,19], but it has several disadvantages: it stains cellulose, which is not abundant in the walls of brown algae [20–22]. In addition, its excitation wavelength corresponds to UV, whose penetration into living tissues is hampered by light scattering and the high radiation energy level results in significant phototoxicity. Many vital probes are available on the market. However, they often miss their targets in brown algae: despite their morphological resemblance to plants, brown algae are phylogenetically very distant from them [23,24]. This specific evolutionary

history confers specific features and components to brown algal cells, making vital probes commonly used in land plants to label the cell contours inefficient. For example, propidium iodide stains the CW in land plants, but labels the nucleus of brown algal cells.

To observe the contours of brown algal cells in 3D over several days, we developed the fluorescent vital probe SBIS, which labels the plasma membrane. Here, we show how this probe can be used to monitor the different cell shapes, sizes and growth modes in three species of brown algae, *Sphacelaria*, *Saccharina* and *Ectocarpus*, using confocal and light-sheet microscopy.

Results

Chemical and optical characteristic of SBIS

Fluorescently labeling the plasma membrane (PM) has become relatively common in animal as well as plant cells [25]. In particular, we have contributed to this field by developing efficient PM fluorescent markers of various colors, such as the MemBright® family [26,27] and others [28,29]. These markers can be used in cells and tissues across various microscopy modes including two-photon imaging [26] and super resolution microscopy, e.g. single molecule localization microscopy (SMLM) [26] and stimulated emission depletion (STED) microscopy [29]. Our strategy relies on functionalizing a fluorescent dye with an amphiphilic and zwitterionic moiety that mimics lipids and efficiently anchors in the cell lipid bilayer [26]. However, this strategy cannot be applied to labeling the PM of marine organisms. The high ionic strength of seawater causes the aggregation and precipitation of these lipophilic probes before they reach their target. Moreover, the thick polar CW of brown algae acts as a shield, preventing the amphiphilic probes from accessing the PM. Therefore, developing such a PM probe is challenging.

To tackle this challenge we synthesized a series of orange-emitting styryl dyes with various degrees of lipophilicity. They were chosen for their ease of synthesis and adjustment [30,31]; several PM probes including the Fei-Mao (FM) dye family [32] and their improved version [29] are based on this fluorescent scaffold.

We first evaluated their ability to label the PM of brown algae using epifluorescence microscopy. Among these tested dyes, one demonstrated efficient PM labeling in brown algae: styryl benzoIndolenium sulfonate, SBIS (Figure 1A).

Comparing the structure of SBIS to the other tested dyes revealed that neutralizing the positive charge of the styryl dye with a sulfonate group significantly improved PM labeling ability. Unlike the classical linear structure of a lipid mimic composed of a lipophilic tail and a polar head (like FM dyes; Figure 1A, left), SBIS has a "T" shape with a lipophilic dye and an orthogonally positioned polar head (Figure 1A, right). Interestingly, when the benzoindolenium moiety was replaced with a quinolinium moiety, the resulting linear amphiphilic probe SQS (Figure 1A, center) failed to stain the PM, suggesting that the orientation of the probe in the bilayer is a key parameter for effective PM targeting. These

observations are in line with a recent study reporting that, for plant cell imaging, T-shaped fluorophores are more efficient than linear ones for staining the PM [33].

Following these initial investigations, the photophysical properties of SBIS were characterized in various environments and their absorption and emission spectra were recorded (Figure 1B & C). Compared to other styryl dyes, SBIS displayed unique properties. First, SBIS possesses much higher molar extinction coefficients (e) than similar styryl dyes (with an aniline donor moiety) like FM1-43 or other styryl dyes we previously developed [29]. In particular, although those dyes possess an e around 50,000 $M^{-1}.cm^{-1}$, that of SBIS ranged between 105,000 (in seawater) and 150,000 $M^{-1}.cm^{-1}$ in dioxane (Figure 1D). Additionally, SBIS exhibited sharp emission peaks with full width at half maximum (FWHM) ranging from 49 to 55 nm, whereas classical styryl dyes exhibit broad excitation bands with FWHM ranging from 80 to 100 nm. Finally, SBIS has a small Stokes shift as low as 28 nm (in dioxane), but styryl dyes are usually characterized by their large Stokes shifts (>100 nm), complicating their use in multicolor imaging. The absorption spectra of SBIS in seawater indicate that SBIS is not prone to aggregation which could be detrimental in imaging.

Interestingly, although SBIS is virtually non-emissive in aqueous media (φ_{Fl} = 0.01), a fluorescence enhancement of 18-fold was observed in non-polar dioxane (Figure 1C), accompanied by a quantum yield of fluorescence (φ_{Fl}) of 0.15. In glycerol, a highly viscous polar solvent, SBIS displayed a 43-fold fluorescence enhancement compared with water (Figure 1C) and reached a quantum yield of fluorescence of 0.48.

Importantly, although SBIS is highly excitable at 560 nm, it is virtually non-excitable at 640 nm (Figure 1B). These wavelengths correspond to two commonly used laser lines in fluorescence bioimaging. Hence, SBIS holds promise for use in multicolor imaging with a far-red fluorescent probe.

Overall, SBIS is an orange-emitting dye with outstanding properties similar to those of rhodamine or cyanine dyes rather than styryl dyes, making it highly suitable for bioimaging. Although SBIS is poorly emissive in seawater, it displays high fluorescence enhancements in non-polar and viscous media, which are important features for the efficient staining of the PM of brown algae and for achieving high signal-to-noise imaging.

SBIS specifically labels the plasma membrane of living *Ectocarpus* sp. cells

Fluorescent probes have become powerful tools to visualize specific cell structures *in vivo*. In brown algal cells, the CW and the PM are located next to each other. To guarantee the specificity of SBIS labeling, we conducted a plasmolysis experiment to detach the PM from the CW in living *Ectocarpus* cells labeled with SBIS and CFW. Plasmolysis revealed that SBIS specifically labeled the PM, compared with CFW which labeled the CW (Figure 2A). SBIS also appears to stain fine structures in the PM: in *Ectocarpus*, we even observed labeled plasmodesmata, which are cytoplasmic bridges between two cells (Figure 2B).

In vivo live imaging of developing organisms requires that the cells remain alive during the imaging process. However, labeling with fluorochromes may be invasive to the organism. To test the effect of SBIS on brown algal development, we used *Ectocarpus* whose growth

rate is about one cell division per day [34]. After labeling *Ectocarpus* with CFW and washing out the fluorochrome, *Ectocarpus* was left to grow for five days in the presence of SBIS. After five days, newly formed cells (lacking CFW labeling) cultured in seawater containing only SBIS showed an SBIS-labeled PM and auto-fluorescent red chloroplasts, which attests to their good condition and that SBIS is not toxic (Figure 2C). Interestingly, when SBIS was washed out of the culture medium before cultivation for five days, we still observed a weak signal corresponding to SBIS in the newly formed cells (Figure 2D). This signal persistence indicates that SBIS may freely diffuse within the membrane to stain the PM of newly formed cells, or may be recycled in the PM. Alternatively, we cannot exclude that a very small amount of SBIS remaining in the medium was enough to label the PM.

Therefore, SBIS can label the PM and be used for monitoring *Ectocarpus* development *in vivo* and over time.

SBIS labeling of the brown algal plasma membrane is stable

In this study, we compared the labeling of known commercial PM fluorochromes, i.e. DID, FM1-43 and FM4-64, with SBIS in three brown algae: *Ectocarpus* sp., *Saccharina latissima* and *Sphacelaria rigidula*. We used CFW as a reference to visualize the CW. DID (DiIC18(5) solid (1,1'-dioctadecyl-3,3,3',3'-tetramethylindodicarbocyanine, 4-chlorobenzenesulfonate salt) is a far-red fluorescent lipophilic carbocyanine with strong fluorescence when incorporated into membranes. In contrast to SBIS (Figure 3A,C,E top panel), DID did not label the PM of *Ectocarpus, Saccharina* or *Sphacelaria* cells (Figure 3A,C,E respectively, second panel from the top) and co-localized with the auto-fluorescent signal emitted from the chloroplasts (far-red emission signal). We also tested FM styryl dyes, which are widely used for imaging PM and early processes of PM internalizsation characterized by endocytosis. In contrast to SBIS, FM4-64 ((N-(3-triethylammoniumpropyl)-4-(6-(4-(diethylamino) phenyl) hexatrienyl) pyridinium dibromide) labeled the PM, but became internalized almost immediately in *Ectocarpus* and within a few minutes in *Saccharina* and *Sphacelaria* (Figure 3A,C,E, respectively; third row of images). Similarly, the styryl dye FM1-43 (N-(3-triethylammoniumpropyl)-4- (4-(dibutylamino) styryl) pyridinium dibromide)) labeled the PM and was quickly internalized by the cells of the cells of the three algae (Figure 3A,C,E, respectively, last row of images). Altogether, our results show that SBIS labels the PM of brown algae cells and, unlike DID, FM4-64 and FM1-43, is not internalized during acquisition (Figure 3A,C,E). Furthermore, we showed that SBIS remains in the PM for at least 8 days, during which the alga remained alive, as attested by the emission of the expected red light from chloroplasts (Figure 3B,D,F).

SBIS labeling combined with confocal, Airyscan or light-sheet microscopy, enables the observation of the 3D shape of brown algal cells

A major bottleneck to study brown algal cell growth is to observe the shape of these cells in their thickness (third axis). High levels of fucoxanthin pigments are present in the chloroplasts of living algal cells, which reflect or scatter light, resulting in poor laser beam penetration within the cells and poor light reflection to the microscope detector. Hence, we

tested the suitability of SBIS for 3D live cell imaging in brown algae, using confocal and light-sheet microscopy. *Ectocarpus* is a brown alga growing only in the X axis, meaning in one dimension, with a cell thickness of 7 µm. Our results show that in confocal microscopy, SBIS allows a clearer visualization of the PM of *Ectocarpus* cells (Figure 4A) and *Saccharina* cells (Figure 4B), compared with CFW labeling. The use of SBIS to mark the PM in its entirety in the X, Y and Z planes, makes it possible to visualize in 3D the location of cell components such as chloroplasts. In addition, SBIS can be used to label the contours of cells, so that shapes can be identified (Figure 4C). Using the Airyscan mode, we gained resolution on the SBIS signal in all three planes (X, Y, Z). In addition, the total noise signal was reduced (Figure 4D). However, chloroplasts were also excited by the laser (561 nm) and Airyscan cannot distinguish between the two emitted signals. Therefore, SBIS may not be useful in the Airyscan acquisition mode when imaging cell thickness in algal cells with many chloroplasts located along the PM, such as in *Saccharina* and *Sphacelaria* cells.

In the brown algae *Saccharina* and *Sphacelaria*, growth in thickness (Z-axis) takes place before relatively long plateau periods of growth initially restricted in the X or the X, Y axes. *Saccharina* initiates growth in the Z-axis in a tissue named the transition zone (TZ), which is located at the base of the lamina [11]. It leads to the formation of a meristoderm that expands in thickness during maturation. Due to their location in thick tissue, imaging cells in the TZ is extremely challenging. We mounted *Saccharina* embryos in the light-sheet and focus on imaging the TZ with the acquisition of z-stacks (Figure 5Aa). Orthoslice views in the X-Y axes through the TZ showed that the CFW signal was visible mainly in the outer cell wall and a few µm into the internal, anticlinal cell walls (Figure 5Ab, Z-axis shown in middle panel outlined in blue, X-Y plane in the middle panel outlined in pink). In comparison, SBIS was able to label the PM of the cells in the TZ, allowing us to distinguish the cell shape of at least the outermost layer of cells (z-stack outlined in blue and orthoslice outlined in pink, showing up to two layers of cells, Figure 5Ab, LUT on SBIS, right-handed side panel). SBIS clearly enhanced the visualization of cells located deeper in the TZ of the *Saccharina* lamina. *Sphacelaria* also develops a 3D tissue through successive and perpendicular longitudinal cell divisions of the subapical cell. Hence, new transverse membranes located deeper inside the tissue are produced along the filament (schematized in Figure 5Ba). Our results show that SBIS, unlike CFW, was able to label the PM of the first cell dividing in 3D (Figure 5Bb). Then, 202 µm further down along the filament, SBIS was able to display transverse PM resulting from an additional longitudinal cell divisions (Figure 5Bc).

Taken together, our results demonstrated that SBIS is a powerful fluorescent probe for *in vivo* 3D imaging of brown algal cell contours in multicellular tissues.

Discussion

Brown algae are ubiquitous macroscopic marine organisms, yet very little is known about the mechanisms involved in their growth [3]. From embryogenesis on, they can develop

complex tissues in the form of embryos comparable to those of animals and plants in their primary architecture, as do the algae of the order Fucales [35,36]. Others grow in successive stages, during which cell growth and division take place in only one orientation, before switching to another spatial dimension, resulting in thicker tissue [37,38]. In this respect, we recently showed that the cells of the embryonic lamina of the kelp *Saccharina latissima*, in order to initiate growth in thickness, first elongate perpendicularly to the surface of the lamina until they reach ~30 µm in length, before dividing parallel to this surface [11]. To identify the process that controls growth orientation during the embryogenesis of these organisms, and more specifically the transition from 2D to 3D growth, it is essential to be able to visualize changes in cell shape in 3D over time, as done in land plant embryos [39].

However, CFW, which labels the cellulose present in the CW, cannot be used to image living brown algal cells thicker than 7 µm using confocal microscopy. Propidium iodide, often used to delineate the outline of plant cells, only stains the nucleus of brown algal cells, as in animals. We have also shown that the FM4-64 and FM1-43 plasma membrane markers internalize quickly and do not allow the cell outline to be imaged for more than a few minutes. In the kelp *Nereocystis luetkean,* another lipophilic fluorescent dye, DiOC6 (3,3′-dihexyloxacarbocyanine iodide; Molecular Probes, Novato, CA, USA), was shown to label the intracellular membranes [40] with excitation and emission spectra (488/505 nm) distinct from CFW and chloroplast auto-fluorescence. However, it was not shown whether DiOC6 was capable of remaining in the PM of living cells for several days or if it was phototoxic [41].

Here, we identified and characterised SBIS, a new fluorescent probe that stably stains the contours of brown algal cells in 3D using both confocal and light-sheet microscopy. SBIS remains localized in the PM for at least 8 days, making the monitoring of cell growth and division possible during algal development. FM4-64 has been reported to be internalized in several studies in brown algae, especially *Fucus* (e.g. [42] and *Sphacelaria* (e.g. [43]) and here we show that FM1-43 internalizes even faster than FM4-64 in brown algal cells. The reasons why SBIS escapes internalization are obscure and, in general, cellular trafficking of fluorescent probes escapes straightforward explanations. The charges and hydrophobicity of the probe likely play an important role. For example, for the same plasma membrane target, uncharged BODIPY-based probes [27] offer much more persistent membrane labelling than positively charged cyanine-based probes [26]. In our study, FM1-43 is doubly negatively charged, whereas SBIS is zwitterionic and therefore neutral overall. Also, as described above, SBIS has a different geometry from the other probes, which may also affect its internalisation.

These differences in charge and spatial conformation may explain why some probes are internalized and others are not. In particular, in other organisms, internalization of extracellular cargos follows two endocytosis pathways, one depending on clathrin proteins [44] and the other one through the formation of caveolae involving proteins such as caveolin and cavins [45]. Selective internalization depends on specific membrane nanodomains [46] that in some cases have been reported to contain specific proteins and lipids such as sphingolipids and cholesterol present on the surface of the plasma membrane [47]. A non-interaction of SBIS with these specific proteins or lipids might explain why SBIS is not internalized. In brown algae, the fast (a few minutes), selective

internalisation of FM1-43 (and of FM4-64 to a lesser extent) compared with the long-lasting maintenance of SBIS on the cell surface is most likely based on clathrin-dependent mechanisms, because homologs of members of this protein machinery are present in the genome of brown algae, in contrast to caveolins and cavins (BLAST search in BOGAS *Ectocarpus* genomics database (https://bioinformatics.psb.ugent.be/orcae/overview/Ectsi [48] and the Phaeoexplorer database for 40 brown algal genomes; https://phaeoexplorer.sb-roscoff.fr/home/ [10]).

The diversity of endocytotic mechanisms that has been illustrated in animals, plants and yeast [44,46,49] opens the door to the possibility that brown algae have developed specific alternative mechanisms, in addition to the clathrin-dependent pathway.

Furthermore, the spectrum of SBIS does not overlap that of chloroplast auto-fluorescence or CFW, which offers the possibility of imaging a third cellular component, i.e., the PM, in addition to the CW and chloroplasts. This aspect is particularly interesting because chloroplasts are often pressed against the PM of brown algal cells and, due to the low Stokes shift of SBIS, they can be distinguished from each without overlaping. SBIS can be thus used in combination with a blue, green and red fluorochrome to obtain multicolor images using separate channels, revealing several structures in the cell.

With the aim of imaging the cellular forms of brown algae over time, SBIS complements the CarboTag marker, which was recently developed to stain the pectins in land plant CWs, and which, surprisingly, stains the pectin-free wall of brown algae [50]. This example further suggests that the identification of vital fluorescent probes for imaging brown algal cells may require an empirical approach, and testing a wide range of candidate molecules.

SBIS will now enable 4D imaging of cells during the embryogenesis of brown algae, making the growth dynamics and geometry accessible to quantification. These data will feed mechanical models that simulate the formation of 3D tissues in brown algae, which has never been undertaken before. However, mechanical modeling of *Ectocarpus* tip growth [16] and cell rounding [12] has already laid the groundwork. To obtain cell size and shape in 3D over time, the images obtained from *Ectocarpus*, *Saccharina* and *Sphacelaria* will need to be processed by image analysis software. In addition to existing 3D reconstruction software, automated image analysis and segmentation algorithms based on deep learning are being developed specifically for brown algae images.

Materials and methods

Preparation of SBIS

Materials for probe synthesis

All starting materials for synthesis were purchased from Sigma-Aldrich, BLD Pharm or TCI Europe and used as received unless stated otherwise. All the synthesized compounds were monitored on TLC (silica) and purified using silica gel columns on a Puriflash 520X+

(Interchim). NMR spectra were carried out on 400 and 500 MHz Bruker Advance II spectrometers. The ^{1}H and ^{13}C NMR chemical shifts are reported relative to residual solvent signals. Data are presented as follows: chemical shift (ppm), multiplicity (s = singlet, d = doublet, t = triplet, q = quartet, p = pintet, dd = doublet of doublets, m = multiplet, br = broad), coupling constant *J* (Hz) and integration. Mass spectra were obtained using an Agilent Q-TOF 6520 mass spectrometer and the MALDI-TOF spectra were collected on a Bruker Autoflex II TOF/TOF mass spectrometer (Bruker Daltonics, Billerica, MA, USA).

Spectroscopy

Milli-Q water (Millipore) and artificial seawater (marine sea salt: Tropic Marin Classic Meersalz) were used for spectroscopy. All the solvents were spectral grade. Absorption and emission spectra were recorded at 20˚C on a Cary 4000-HP spectrophotometer (Varian) and a FluoroMax-4 spectrofluorometer (Horiba Jobin Yvon) equipped with a thermostated cell compartment, respectively. For standard recording of fluorescence spectra, emissions were collected 10 nm after the excitation wavelength. All the spectra were corrected from the wavelength-dependent response of the detector. The fluorescence quantum yields ϕ_{Fl} were determined from the following equation:

$$\phi_{Fl} = \phi_{ref} \times \frac{I_{fluo}^{sample}\, d\lambda}{I_{fluo}^{ref} d\lambda} \times \frac{OD_{ref}}{OD_{sample}} \times \frac{n_{sample}^2}{n_{ref}^2}$$

where OD is the optical density at the excitation wavelength, and η the refraction index of the solvent. Rhodamine B was used as the reference (in water, f_{Fl}= 0.31) [51]. The oil mixtures were prepared as follows: 1 g of the appropriate oil ratio was heated to 50°C. 5 µL of a 200 µM solution of the dye in dioxane was added and the mixture was homogenized manually. The samples were cooled down at room temperature before being analyzed.

Synthesis of SBIS

3-(1,1,2-trimethyl-1*H*-benzo[*e*]indol-3-ium-3-yl)propane-1-sulfonate **1** was synthesized according to a protocol described in the literature [52].

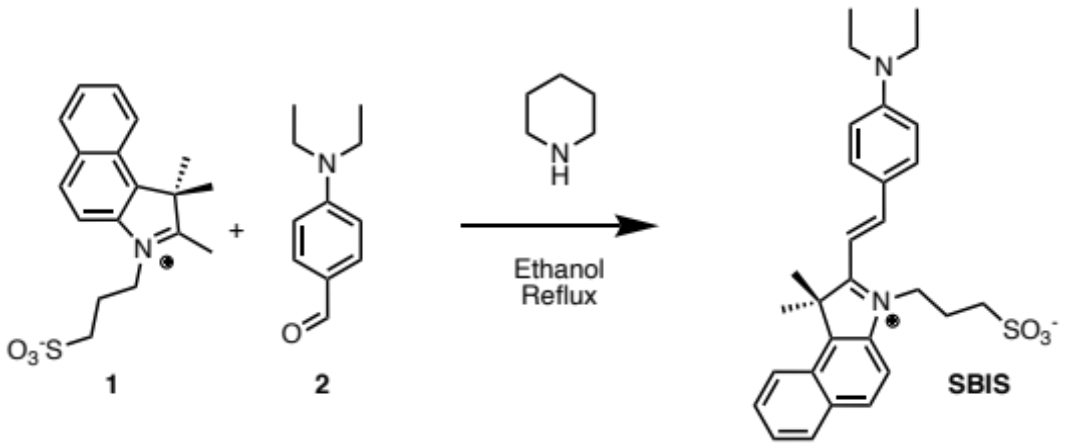

Piperidine (0.5 mL) was added to a solution of 3-(1,1,2-trimethyl-1*H*-benzo[*e*]indol-3-ium-3-yl)propane-1-sulfonate **1** (500 mg, 1.51 mmol) and 4-(diethylamino)benzaldehyde **2** (320 mg, 1.81 mmol, 1.2 eq) in absolute ethanol (30 mL) . The solution was refluxed at 110°C and rapidly turned dark violet. The reaction was allowed to reflux for 1 h before being cooled down to room temperature. The solvents were evaporated under reduced pressure and the crude fraction was purified by column chromatography on silica gel (DCM:MeOH, 99:1 to 9:1) to obtain 350 mg of SBIS as a dark violet solid (Yield, 47%). Rf = 0.38 (DCM:MeOH, 9:1).

^{1}H-NMR (400 MHz, MeOD): δ 8.40 (d, *J* = 15.5 Hz, 1H, CH ethylene), 8.35 (d, *J* = 8.5 Hz, 1H), 8.16 (d, *J* = 8.9 Hz, 1H), 8.10 (d, *J* = 8.5 Hz, 1H), 8.09-8.05 (m, 2H), 7.92 (d, *J* = 8.9 Hz, 1H), 7.74 (ddd, *J* = 8.4, 7.0, 1.3 Hz, 1H), 7.62 (ddd, *J* = 8.1, 7.0, 1.0 Hz, 1H), 7.45 (d, *J* = 15.5 Hz, 1H, , CH ethylene), 6.92 (d, *J* = 9.2 Hz, 2H), 4.81 (t, *J* = 8.2 Hz, 2H, CH_2-N^+), 3.61 (q, *J* = 7.1 Hz, 4H, 2 CH_2 Et), 3.10 (t, *J* = 6.3 Hz, 2H, CH_2), 2.42 (tt, *J* = 9.6, 5.0 Hz, 2H, CH_2), 2.08 (s, 6H, 2 CH_3 Me), 1.29 (t, *J* = 7.1 Hz, 6H, 2 CH_3 Et).

^{13}C-NMR (101 MHz, MeOD): δ 190.62, 180.50, 154.31, 153.61, 138.87, 136.32, 133.09, 130.90, 129.83, 127.74, 127.58, 125.95, 122.50, 122.30, 112.12, 111.53, 103.21, 52.65, 44.70, 43.92, 31.62, 25.90, 22.31, 11.52.

HRMS (ESI$^+$), calculated for $C_{29}H_{35}N_2O_3S^+$ $[M+H]^+$ 491.2363, found 491.2387

Culture of algae

Ectocarpus sp. material was produced from fragmentation of the WT male strain Ec32 (CCAP 1310/4; origin San Juan de Marcona, Peru) parthenosporophytes.

Embryos of *Saccharina latissima* were produced from fertilization of the female gametophyte strain F1 with the male strain M1 as described in [38]. Female gametophytes of *Sphacelaria rigidula* were grown from fragmentation of adult cultures. All alga thalli were

grown in full-strength Provasoli-enriched [53] autoclaved natural or artificial seawater (pH 7.8) (Tropic Marin®) in a culture cabinet at 13°C with a 12:12 light: dark cycle (light intensity, 29 µmol photon·m^{-2}·s^{-1}) as described in [54].

Fluorochromes

Brown algae were labeled with Calcofluor White (ref BCCK5631 from Sigma-Aldrich ®) at 10 µM, SBIS at 5 µM, DID at 10 µM, FM6-64 at 10 µM, FM1-43 at 10 µM, in seawater overnight at 13°C and washed 3 times in seawater and 13°C the next morning. DAPI was used at 20 µM for 1.5 h at 13°C and then washed 3 times in seawater. DID (ref. D7757), FM6-64 (ref. T3166) and FM1-43 (ref. T3163) were purchased from ThermoFisher Scientific®. DAPI (ref. D9542) was purchased from Sigma-Aldrich®. The excitation and emission spectra of the different probes are as follows: DAPI: 340/488 nm; CFW: 405/432–457 nm; SBIS: 560/610 nm; FM1-43: 488/590 nm; FM4-64 : 488–514 /625–670 nm; DID: 650/650–700 nm; chlorophyll A (Chloroplasts): 430–561 / 650–700 nm.

Confocal microscopy

Brown algae were imaged on a Zeiss LSM 880 confocal microscope equipped with an NLO Airyscan 1 using a LD C-Apochromat 40x/1.1 W Korr M27 objective. *Ectocarpus*, *Saccharina* and *Sphacelaria* were mounted in a 20 mm diameter glass-bottom cell culture dish, glass of standard thickness 0.16-0.19mm (Cat. No. 801001) filled with seawater. For every alga, co-labeling of CFW + SBIS or DID or FM4-64 or FM1-43 was performed on the same day and imaged in the same glass-bottom cell culture dish.

Light-sheet microscopy

Brown algae were imaged on a Zeiss Lightsheet 7 microscope using a W Plan-Apochromat 20x/1.0 DIC M27 objective. *Saccharina* was mounted in 1% low melting agarose (ref SLCN4676 from Sigma-Aldrich ®) in seawater and *Sphacelaria* was glued (ref. 62928642 from Leroy Merlin ®) onto a glass capillary.

Imaging: software used for 3D image reconstruction

Z-stacks and snaps taken on the LSM880 and LS7 in their native format (.czi) were visualized in Fiji (open source, available at http://fiji.sc/Fiji; [55]), Zen Blue (Carl Zeiss Microscopy, LLC) and Imaris 10.2.0 (BitPlane, South Windsor, CT, USA).

Acknowledgements

We thank Tanguy Dufourt for the initial labeling experiments. Part of the work was funded by the European Union (ERC, ALTER e-GROW, project number 101055148). Views and opinions expressed are those of the author(s) only and do not necessarily reflect those of

the European Union or the European Research Council Executive Agency. Neither the European Union nor the granting authority can be held responsible for them. For purposes of open access dissemination, the authors applied for a CC BY-NC license for this document.

Contribution

M.C. produced SBIS and M.Z. designed and carried out all the image acquisitions. M.C, M.Z. and B.C. directed the work and wrote the article. All the authors read and approved the manuscript.

References

1. Arkema KK, Reed DC, Schroeter SC. Direct and indirect effects of giant kelp determine benthic community structure and dynamics. Ecology. 2009;90: 3126–3137. doi:10.1890/08-1213.1
2. Barbier M, Araújo R, Rebours C, Jacquemin B, Holdt SL, Charrier B. Development and objectives of the PHYCOMORPH European Guidelines for the Sustainable Aquaculture of Seaweeds (PEGASUS). Botanica Marina. 2020;63: 5–16. doi:10.1515/bot-2019-0051
3. Charrier B, Le Bail A, de Reviers B. Plant Proteus: brown algal morphological plasticity and underlying developmental mechanisms. Trends in Plant Science. 2012;17: 468–477. doi:10.1016/j.tplants.2012.03.003
4. de Groot R, Brander L, van der Ploeg S, Costanza R, Bernard F, Braat L, et al. Global estimates of the value of ecosystems and their services in monetary units. Ecosystem Services. 2012;1: 50–61. doi:10.1016/j.ecoser.2012.07.005
5. González Fernández LA, Castillo Ramos V, Sánchez Polo M, Medellín Castillo NA. Fundamentals in applications of algae biomass: A review. Journal of Environmental Management. 2023;338: 117830. doi:10.1016/j.jenvman.2023.117830
6. Holdt SL, Edwards MD. Cost-effective IMTA: a comparison of the production efficiencies of mussels and seaweed. J Appl Phycol. 2014;26: 933–945. doi:10.1007/s10811-014-0273-y
7. Hurd CL, Law CS, Bach LT, Britton D, Hovenden M, Paine ER, et al. Forensic carbon accounting: Assessing the role of seaweeds for carbon sequestration. Journal of Phycology. 2022;n/a. doi:10.1111/jpy.13249
8. Krause-Jensen D, Duarte CM. Substantial role of macroalgae in marine carbon sequestration. Nature Geosci. 2016;9: 737–742. doi:10.1038/ngeo2790
9. Malla FA, Malla AA, Bandh SA, Sofi NA, Ahmed M. The Role of Brown Algae in Global Warming Mitigation. In: Kurniawan TA, Anouzla A, editors. Algae as a Natural

Solution for Challenges in Water-Food-Energy Nexus: Toward Carbon Neutrality. Singapore: Springer Nature; 2024. pp. 813–831. doi:10.1007/978-981-97-2371-3_28

10. Denoeud F, Godfroy O, Cruaud C, Heesch S, Nehr Z, Tadrent N, et al. Evolutionary genomics of the emergence of brown algae as key components of coastal ecosystems. Cell. 2024;0. doi:10.1016/j.cell.2024.10.049

11. Theodorou I, Charrier B. The shift to 3D growth during embryogenesis of kelp species, atlas of cell division and differentiation of Saccharina latissima. Development. 2023;150: dev201519. doi:10.1242/dev.201519

12. Jia F, Ben Amar M, Billoud B, Charrier B. Morphoelasticity in the development of brown alga Ectocarpus siliculosus: from cell rounding to branching. J R Soc Interface. 2017;14: 20160596. doi:10.1098/rsif.2016.0596

13. Le Bail A, Billoud B, Maisonneuve C, Peters A, Cock JM, Charrier B. Initial pattern of development of the brown alga Ectocarpus siliculosus (Ectocarpales, Phaeophyceae) sporophyte. Journal of Phycology. 2008;44: 1269–1281.

14. Le Bail A, Billoud B, Le Panse S, Chenivesse S, Charrier B. ETOILE regulates developmental patterning in the filamentous brown alga Ectocarpus siliculosus. Plant Cell. 2011;23: 1666–1678. doi:10.1105/tpc.110.081919

15. Fritsch FE. The Structure And Reproduction Of The Algae. The University Press. Cambridge: Cambridge University Press; 1945.

16. Rabillé H, Billoud B, Tesson B, Le Panse S, Rolland É, Charrier B. The brown algal mode of tip growth: Keeping stress under control. PLoS Biol. 2019;17: e2005258. doi:10.1371/journal.pbio.2005258

17. Muñoz-Miranda LA, Iñiguez-Moreno M. An extensive review of marine pigments: sources, biotechnological applications, and sustainability. Aquat Sci. 2023;85: 68. doi:10.1007/s00027-023-00966-8

18. Wang W-J, Wang G-C, Zhang M, Tseng CK. Isolation of Fucoxanthin from the Rhizoid of Laminaria japonica Aresch. Journal of Integrative Plant Biology. 2005;47: 1009–1015. doi:10.1111/j.1744-7909.2005.00054.x

19. Clerc T, Boscq S, Attia R, Kaminski Schierle GS, Charrier B, Läubli NF. Cultivation and Imaging of S. latissima Embryo Monolayered Cell Sheets Inside Microfluidic Devices. Bioengineering. 2022;9: 718. doi:10.3390/bioengineering9110718

20. Charrier B, Rabillé H, Billoud B. Gazing at Cell Wall Expansion under a Golden Light. Trends Plant Sci. 2019;24: 130–141. doi:10.1016/j.tplants.2018.10.013

21. Deniaud-Bouët E, Hardouin K, Potin P, Kloareg B, Hervé C. A review about brown algal cell walls and fucose-containing sulfated polysaccharides: Cell wall context, biomedical properties and key research challenges. Carbohydrate Polymers. 2017;175: 395–408. doi:10.1016/j.carbpol.2017.07.082

22. Popper ZA, Michel G, Hervé C, Domozych DS, Willats WGT, Tuohy MG, et al. Evolution and Diversity of Plant Cell Walls: From Algae to Flowering Plants. Annual

Review of Plant Biology. 2011;62: 567–590. doi:10.1146/annurev-arplant-042110-103809

23. Burki F, Roger AJ, Brown MW, Simpson AGB. The New Tree of Eukaryotes. Trends in Ecology & Evolution. 2020;35: 43–55. doi:10.1016/j.tree.2019.08.008

24. Silberfeld T, Leigh JW, Verbruggen H, Cruaud C, de Reviers B, Rousseau F. A multi-locus time-calibrated phylogeny of the brown algae (Heterokonta, Ochrophyta, Phaeophyceae): Investigating the evolutionary nature of the “brown algal crown radiation.” Molecular Phylogenetics and Evolution. 2010;56: 659–674. doi:10.1016/j.ympev.2010.04.020

25. Collot M, Pfister S, Klymchenko AS. Advanced functional fluorescent probes for cell plasma membranes. Current Opinion in Chemical Biology. 2022;69: 102161. doi:10.1016/j.cbpa.2022.102161

26. Collot M, Ashokkumar P, Anton H, Boutant E, Faklaris O, Galli T, et al. MemBright: A Family of Fluorescent Membrane Probes for Advanced Cellular Imaging and Neuroscience. Cell Chemical Biology. 2019;26: 600-614.e7. doi:10.1016/j.chembiol.2019.01.009

27. Collot M, Boutant E, Lehmann M, Klymchenko AS. BODIPY with Tuned Amphiphilicity as a Fluorogenic Plasma Membrane Probe. Bioconjugate Chem. 2019;30: 192–199. doi:10.1021/acs.bioconjchem.8b00828

28. Collot M, Kreder R, L. Tatarets A, D. Patsenker L, Mely Y, S. Klymchenko A. Bright fluorogenic squaraines with tuned cell entry for selective imaging of plasma membrane vs. endoplasmic reticulum. Chemical Communications. 2015;51: 17136–17139. doi:10.1039/C5CC06094J

29. Collot M, Boutant E, Fam KT, Danglot L, Klymchenko AS. Molecular Tuning of Styryl Dyes Leads to Versatile and Efficient Plasma Membrane Probes for Cell and Tissue Imaging. Bioconjugate Chem. 2020;31: 875–883. doi:10.1021/acs.bioconjchem.0c00023

30. Li Q, Lee JS, Ha C, Chan BP, Yang G, Wen BG, et al. Solid-phase synthesis of styryl dyes and their application as amyloid sensors. Angewandte Chemie - International Edition. 2004;43: 6331–6335. doi:10.1002/anie.200461600

31. Wuskell JP, Boudreau D, Wei M, Jin L, Engl R, Chebolu R, et al. Synthesis, spectra, delivery and potentiometric responses of new styryl dyes with extended spectral ranges. Journal of Neuroscience Methods. 2006;151: 200–215. doi:10.1016/j.jneumeth.2005.07.013

32. Schote U, Seelig J. Interaction of the neuronal marker dye FM1-43 with lipid membranes: Thermodynamics and lipid ordering. Biochimica et Biophysica Acta (BBA) - Biomembranes. 1998;1415: 135–146. doi:10.1016/S0005-2736(98)00188-6

33. Peng X, Pan J, Han Z, Wu P, He Z, Feng H, et al. Three-dimensional tracking of organ development in live plants based on plasma membrane dyes at single-cell resolution. Spectrochimica Acta Part A: Molecular and Biomolecular Spectroscopy. 2025;329: 125575. doi:10.1016/j.saa.2024.125575

34. Nehr Z, Billoud B, Le Bail A, Charrier B. Space-time decoupling in the branching process in the mutant étoile of the filamentous brown alga Ectocarpus siliculosus. Plant Signal Behav. 2011;6: 1889–1892.

35. Berger F, Taylor A, Brownlee C. Cell fate determination by the cell wall in early fucus development. Science. 1994;263: 1421–1423. doi:10.1126/science.263.5152.1421

36. Brownlee C, Berger F. Extracellular matrix and pattern in plant embryos: on the lookout for developmental information. Trends in Genetics. 1995;11: 344–348. doi:10.1016/S0168-9525(00)89104-0

37. Boscq S, Billoud B, Charrier B. Cell-Autonomous and Non-Cell-Autonomous Mechanisms Concomitantly Regulate the Early Developmental Pattern in the Kelp Saccharina latissima Embryo. Plants. 2024;13: 1341. doi:10.3390/plants13101341

38. Boscq S, Billoud B, Theodorou I, Joemmanbaks T, Dufourt T, Charrier B. MUM, a maternal unknown message, inhibits early establishment of the medio-lateral axis in the embryo of the kelp Saccharina latissima. Development. 2024;151: dev202732. doi:10.1242/dev.202732

39. Laruelle E, Belcram K, Trubuil A, Palauqui J-C, Andrey P. Large-scale analysis and computer modeling reveal hidden regularities behind variability of cell division patterns in Arabidopsis thaliana embryogenesis. Wabnik K, Kleine-Vehn J, editors. eLife. 2022;11: e79224. doi:10.7554/eLife.79224

40. Knoblauch J, Drobnitch ST, Peters WS, Knoblauch M. In situ microscopy reveals reversible cell wall swelling in kelp sieve tubes: one mechanism for turgor generation and flow control? Plant, Cell & Environment. 2016;39: 1727–1736. doi:10.1111/pce.12736

41. Fotopoulos V. Never say dye: New roles for an old fluorochrome. Plant Signaling & Behavior. 2012;7: 342–344. doi:10.4161/psb.19236

42. Belanger KD, Quatrano RS. Membrane recycling occurs during asymmetric tip growth and cell plate formation inFucus distichus zygotes. Protoplasma. 2000;212: 24–37. doi:10.1007/BF01279344

43. Aoki H, Katsaros C, Motomura T, Nagasato C. Simultaneous visualization of the actin plate and new cell partition membrane during cytokinesis in the brown alga Sphacelaria rigidula (Sphacelariales, Phaeophyceae). Phycological Research. 2023;71: 107–115. doi:10.1111/pre.12512

44. Johnson A. Mechanistic divergences of endocytic clathrin-coated vesicle formation in mammals, yeasts and plants. Journal of Cell Science. 2024;137: jcs261847. doi:10.1242/jcs.261847

45. Matthaeus C, Taraska JW. Energy and Dynamics of Caveolae Trafficking. Front Cell Dev Biol. 2021;8. doi:10.3389/fcell.2020.614472

46. Jaillais Y, Bayer E, Bergmann DC, Botella MA, Boutté Y, Bozkurt TO, et al. Guidelines for naming and studying plasma membrane domains in plants. Nat Plants. 2024;10: 1172–1183. doi:10.1038/s41477-024-01742-8

47. Róg T, Vattulainen I. Cholesterol, sphingolipids, and glycolipids: What do we know about their role in raft-like membranes? Chemistry and Physics of Lipids. 2014;184: 82–104. doi:10.1016/j.chemphyslip.2014.10.004

48. Cock JM, Sterck L, Rouzé P, Scornet D, Allen AE, Amoutzias G, et al. The Ectocarpus genome and the independent evolution of multicellularity in brown algae. Nature. 2010;465: 617–621. doi:10.1038/nature09016

49. Tsai Y-T, Moore W, Kim H, Budin I. Bringing rafts to life: Lessons learned from lipid organization across diverse biological membranes. Chem Phys Lipids. 2020;233: 104984. doi:10.1016/j.chemphyslip.2020.104984

50. Besten M, Hendriksz M, Michels L, Charrier B, Smakowska-Luzan E, Weijers D, et al. CarboTag: a modular approach for live and functional imaging of plant cell walls. bioRxiv; 2024. p. 2024.07.05.597952. doi:10.1101/2024.07.05.597952

51. Magde D, Rojas GE, Seybold PG. Solvent Dependence of the Fluorescence Lifetimes of Xanthene Dyes. Photochemistry and Photobiology. 1999;70: 737–744. doi:10.1111/j.1751-1097.1999.tb08277.x

52. Menéndez GO, López CS, Jares-Erijman EA, Spagnuolo CC. A Versatile Near-Infrared Asymmetric Tricarbocyanine for Zinc Ion Sensing in Water. Photochemistry and Photobiology. 2013;89: 1354–1361. doi:10.1111/php.12160

53. Starr RC, Zeikus JA. Utex—the Culture Collection of Algae at the University of Texas at Austin 1993 List of Cultures1. Journal of Phycology. 1993;29: 1–106. doi:10.1111/j.0022-3646.1993.00001.x

54. Le Bail A, Charrier B. Culture Methods and Mutant Generation in the Filamentous Brown Algae Ectocarpus siliculosus. In: De Smet I, editor. Plant Organogenesis. Humana Press; 2013. pp. 323–332. Available: http://dx.doi.org/10.1007/978-1-62703-221-6_22

55. Schindelin J, Arganda-Carreras I, Frise E, Kaynig V, Longair M, Pietzsch T, et al. Fiji - an Open Source platform for biological image analysis. Nature methods. 2012;9: 676–682. doi:10.1038/nmeth.2019

455 **Figure legends**

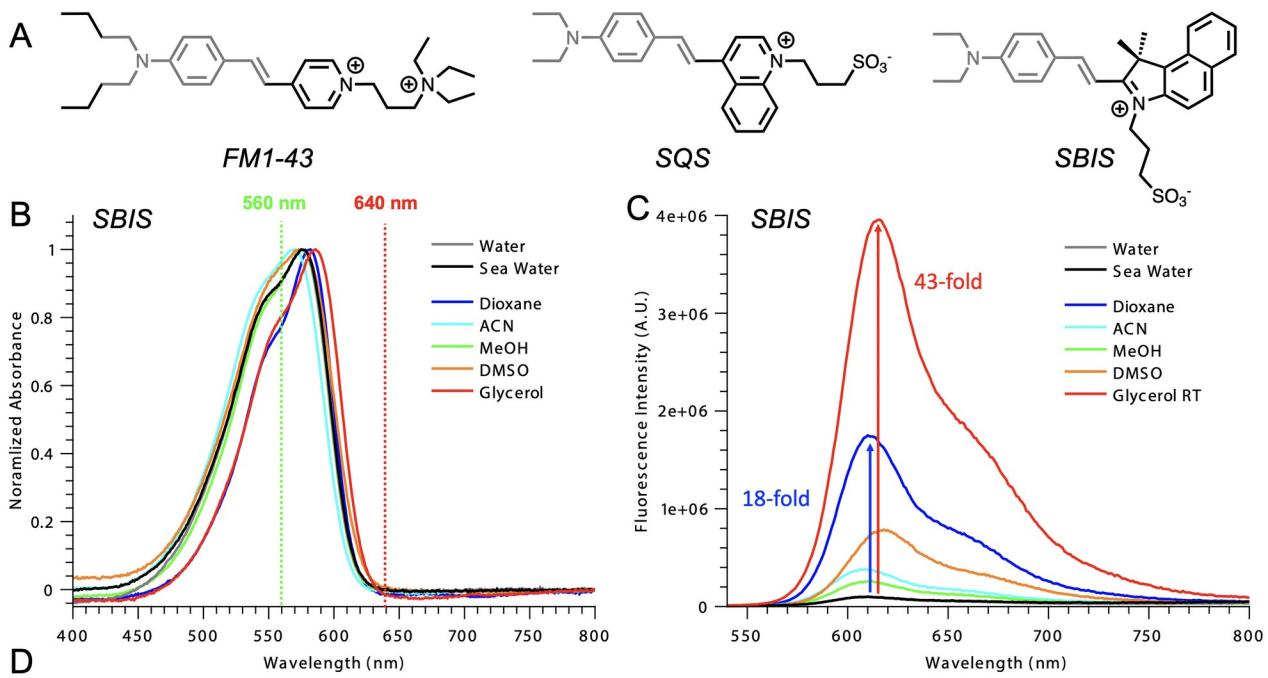

D

Solvent	λAbs max (nm)	excitation @560 nm (% max)	FWHM (nm)	ε ($M^{-1}.cm^{-1}$)	λEm max (nm)	FWHM (nm)	ϕ_{FI}
Dioxane	582	78	68	150,000	610	49	0.15
ACN	570	97	80	122,000	609	50	0.03
MeOH	576	91	76	140,000	612	53	0.02
DMSO	573	95	86	109,000	618	53	0.07
Water	575	91	79	110,000	606	N/A	0.01
Sea Water	575	91	80	105,000	610	N/A	0.01
Glycerol	586	80	73	121,000	616	55	0.48

Figure 1: Structural and photophysical properties of SBIS.

(A) Structures of the styryl dyes discussed in this work. The gray part of the structure is the anillin electron-donor moiety commonly found in the three probes. **(B)** Normalized absorption spectra of SBIS (1 µM) in various solvents. The vertical lines represent the commonly used 560 and 640 nm laser lines. **(C)** Fluorescence intensity of SBIS (1 µM) in various solvents showing the fluorescence enhancement of the dye when placed in a non-polar or viscous environment. Excitation was at 530 nm. **(D)** Photophysical properties of SBIS in the tested solvents.

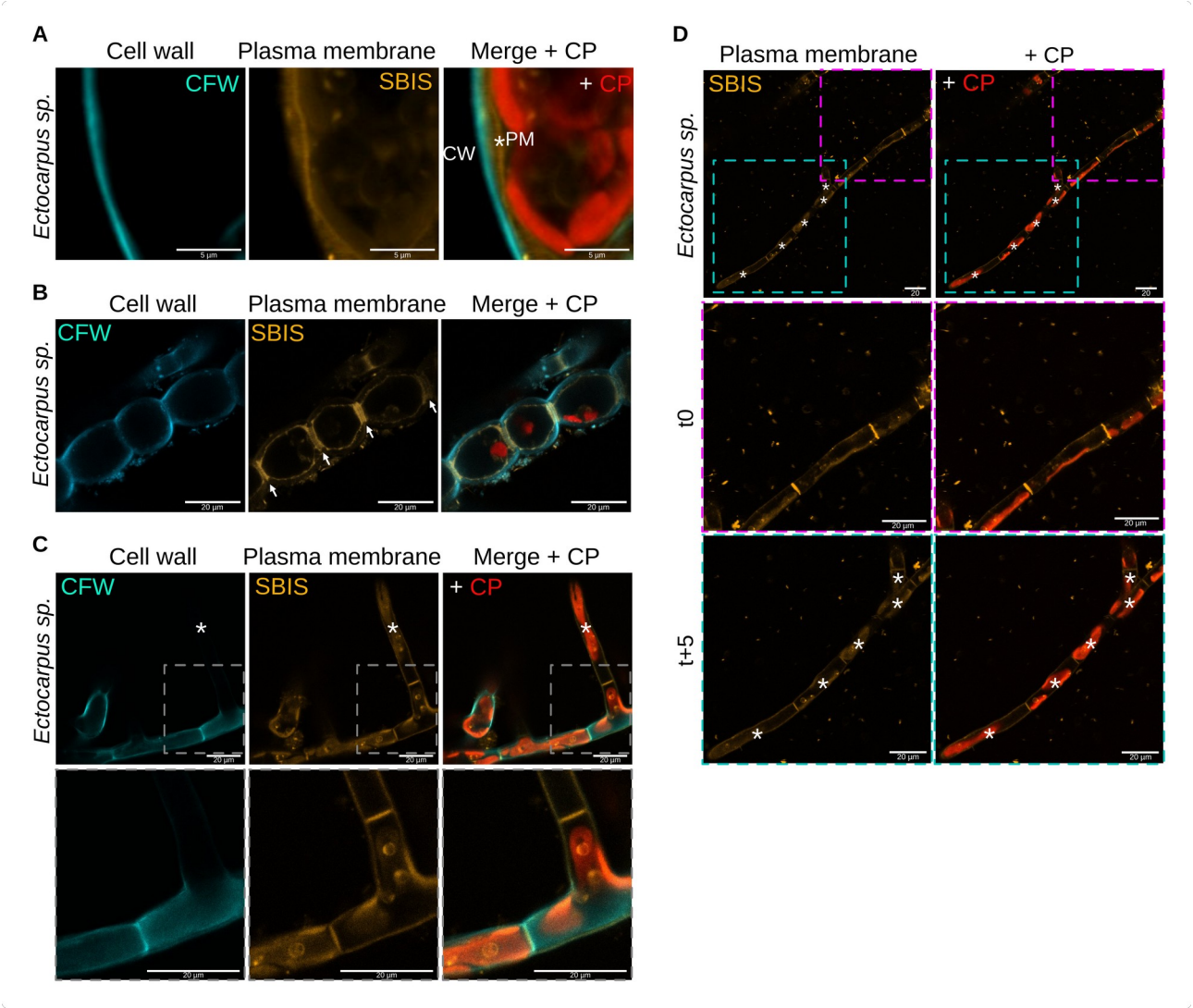

Figure 2: Labeling of the plasma membrane with SBIS.

(A) SBIS labels the plasma membrane (PM) of the brown alga *Ectocarpus sp*. Plasmolysis conducted with 2 M NaCl results in the detachment of the PM (white asterisk) in response to a hyperosmotic stress and reveals the specific labeling of SBIS (orange) on the PM, compared with the labeling of Calcofluor White (CFW, cyan) on the cell wall (CW). **(B)** SBIS allows the labeling of fine structures on the PM, such as plasmodesmata (indicated by white arrows). **(C)** SBIS does not impair the growth of *Ectocarpus*. *Ectocarpus* filaments were labeled with CFW, washed and incubated in SBIS for 5 days. Top: overview of the *Ectocarpus* filament. A branch formed after labeling with CFW and during incubation in SBIS (white asterisk). As expected, the branch is labeled with SBIS only. Bottom: enlargement of the gray-dashed rectangle showing the longitudinal and transverse PM of newly formed cells labeled with SBIS. Auto-fluorescent chloroplasts attest that the cells are alive. **(D)** SBIS accumulates in the PM 5 days after washing. *Ectocarpus* filaments were labeled with SBIS, washed at t0 and grown for 5 days (t+5), newly formed cells are indicated by a white asterisk. Left: only SBIS (orange), Right: SBIS with chloroplast auto-fluorescence (CP, in red). Top: overview of an *Ectocarpus* filament. Middle: *Ectocarpus* filament region already present and labeled at t0 (magenta-dashed square). Bottom: New *Ectocarpus* filament grown for 5 days after removal of SBIS (cyan-dashed square), the 5

newly formed cells are indicated by a white asterisk. The presence of chloroplasts (in red) is an indicator that the cells are in good condition. CFW is excited with a 405 nm laser and the detection band is 410–470 nm (Exc 405/Em 410–470). SBIS: Exc 561/Em 578–632; Chloroplast auto-fluorescence: Exc 561/Em 674–721.

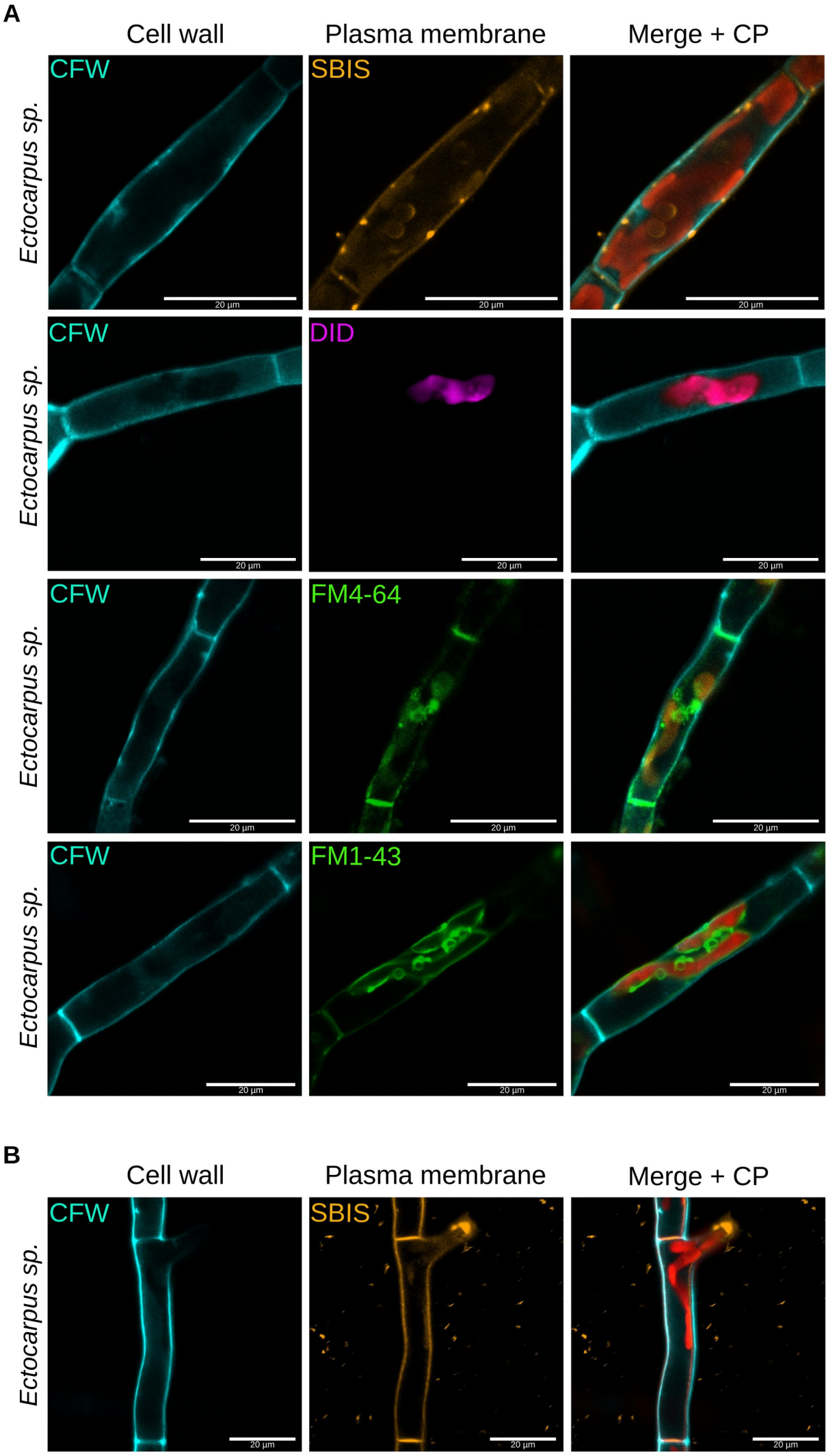
A
Cell wall
Plasma membrane
Merge + CP
Ectocarpus sp.
CFW
SBIS
DID
FM4-64
FM1-43
20 µm
B

C

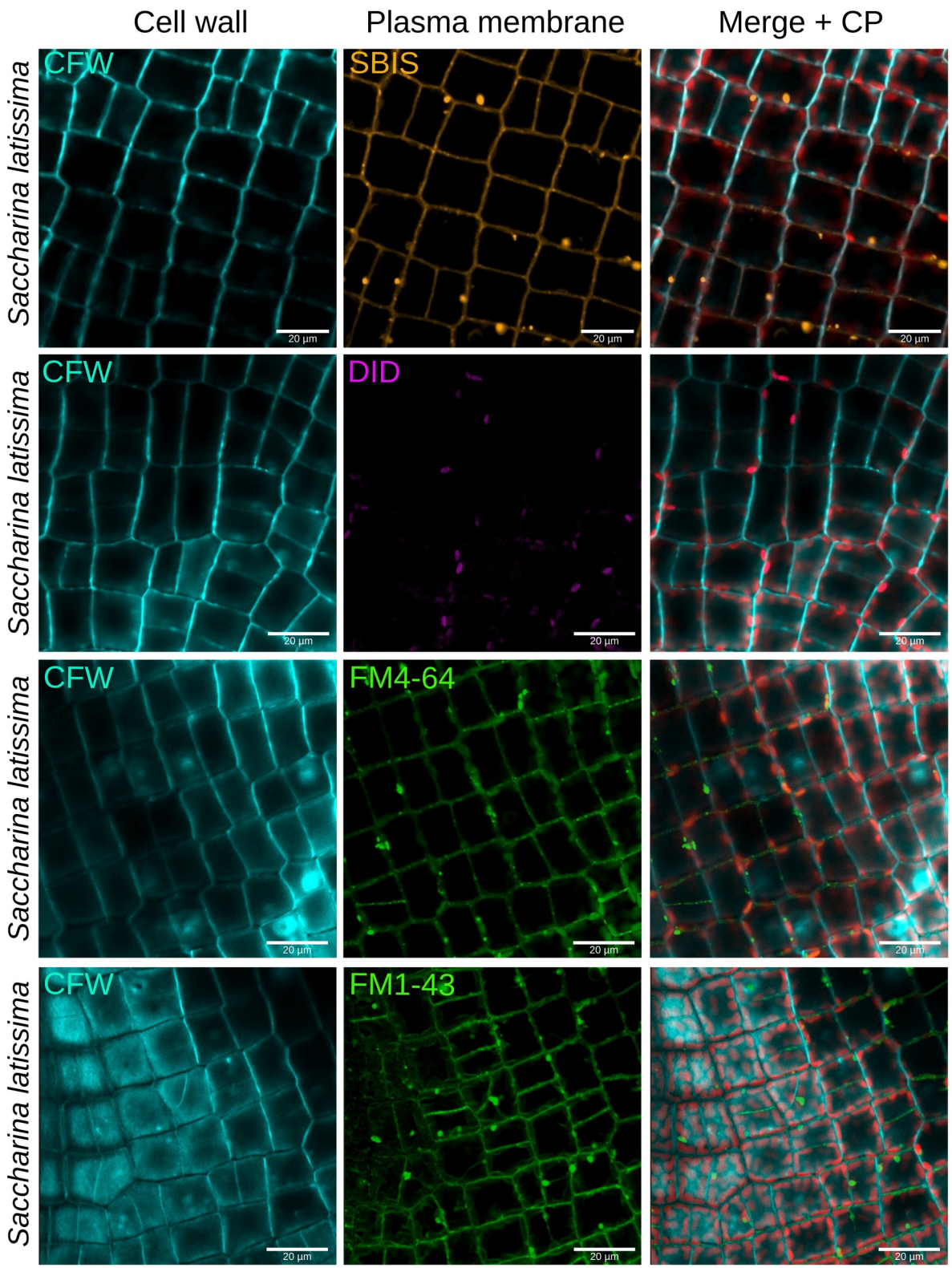
Cell wall
Plasma membrane
Merge + CP
Saccharina latissima
CFW
SBIS
DID
FM4-64
FM1-43
20 µm

D

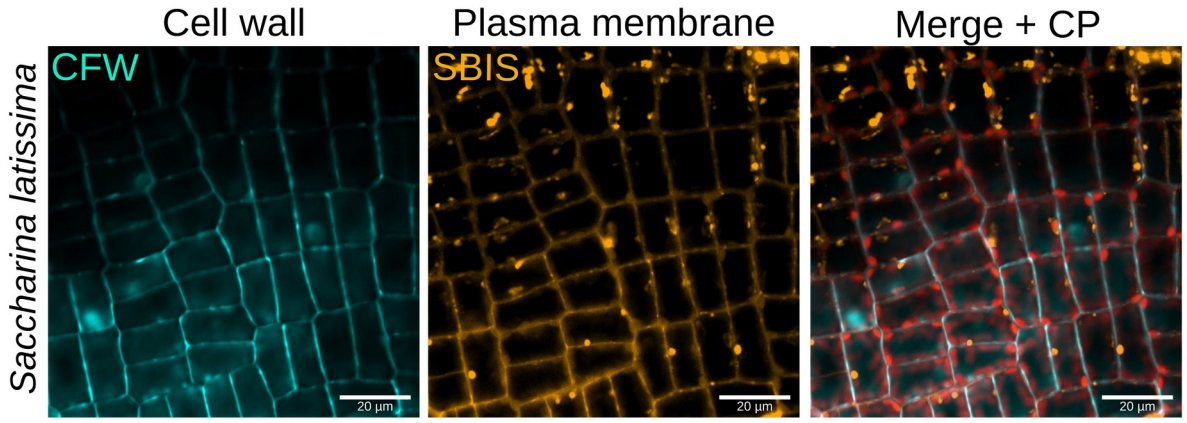
Cell wall
Plasma membrane
Merge + CP
Saccharina latissima
CFW
SBIS
20 µm

E

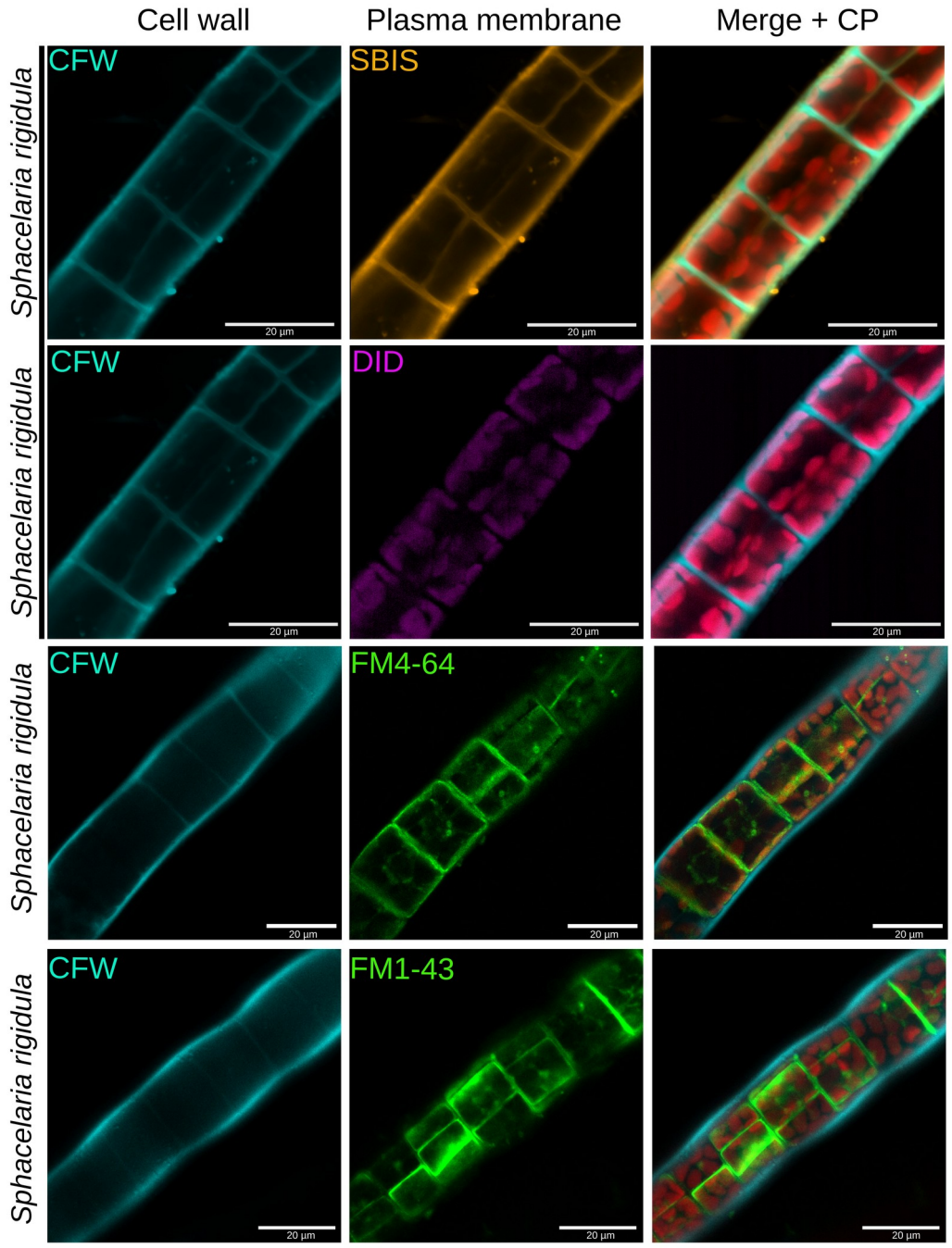
Cell wall
Plasma membrane
Merge + CP
Sphacelaria rigidula
CFW
SBIS
DID
FM4-64
FM1-43
20 µm

F

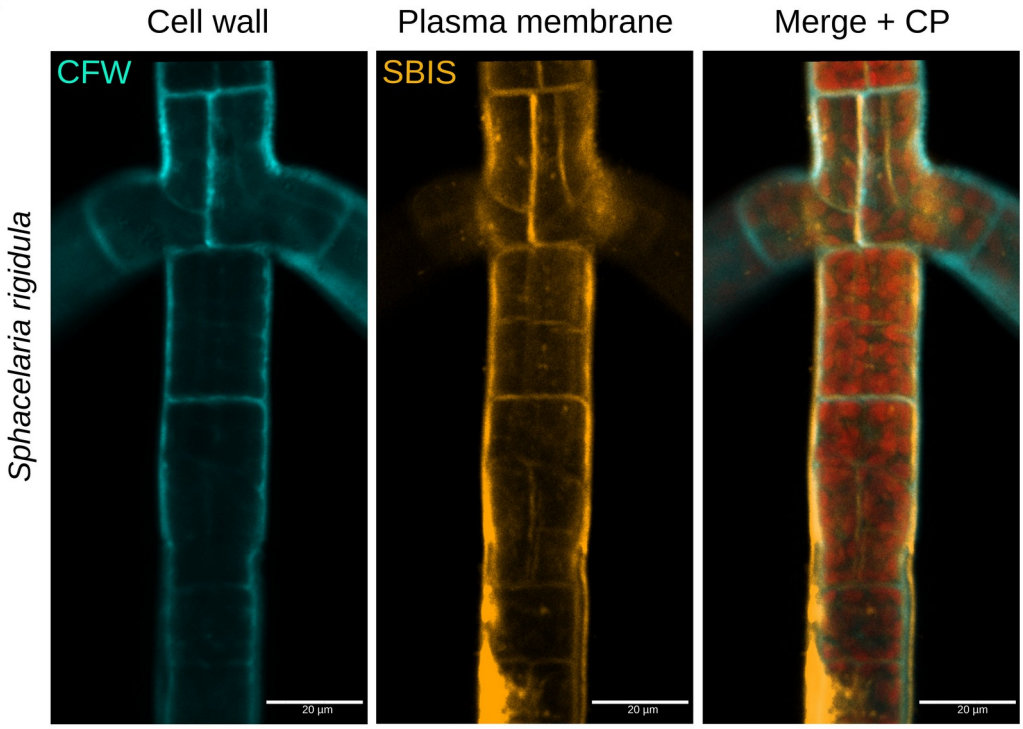
Cell wall
Plasma membrane
Merge + CP
Sphacelaria rigidula
CFW
SBIS
20 µm

Figure 3: Stability of SBIS in the plasma membrane.

Unlike other known plasma membrane (PM) labeling fluorochromes, SBIS is not internalized over time. DID, FM1-43 and FM6-64, were tested in addition to SBIS in three different brown algae: *Ectocarpus* sp., *Sphacelaria rigidula* and *Saccharina latissima*. **(A)** Labeling of the *Ectocarpus* cell PM by SBIS, whereas DID does not stain the PM in *Ectocarpus*. It should be noted that the excitation and emission wavelength ranges of DID are the same as those of chloroplasts, resulting in a co-location of the two signals. FM1-43 and FM6-64 label the PM but get internalized during confocal imaging. **(B)** Long-term retention of SBIS in the PM. SBIS keeps labeling the PM of *Ectocarpus* cells for up to 8 days after SBIS removal by washing. **(C)** In *Saccharina*, the same result is observed as in **(A)**. **(D)** SBIS remains primarily in the PM of *Saccharina* cells for 8 days, but the signal is blurred, suggesting some internalization of the probe. **(E)** In *Sphacelaria*, the same result is observed as in **(A**, **C)**. **(F)** SBIS remains in the PM of *Sphacelaria* cells for up to 8 days. All labeling of PM fluorochromes was done in co-labeling with CFW to label the cell wall. Chloroplasts are visualized in red (auto-fluorescence). CFW is excited (Exc) with a 405 nm laser and the detection (emission Em) band is 410–470 nm. SBIS: Exc 561/Em 578–632; DID: Exc 633/Em 650–700; FM1-43: Exc 488/Em 580–640; FM4-64: Exc 488/Em 561–641; chloroplast auto-fluorescence: Exc 561/Em 674–721.

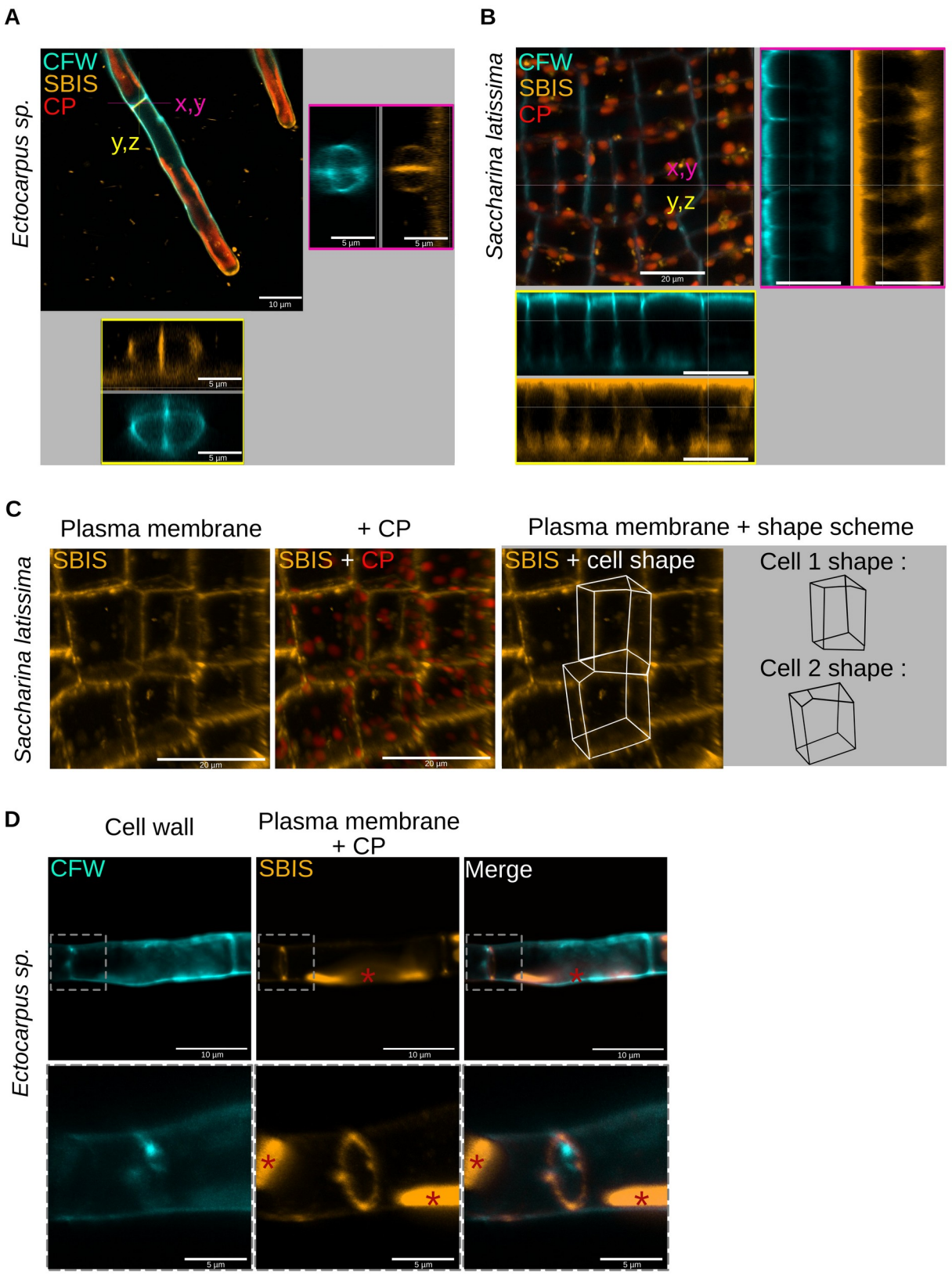

515 **Figure 4: SBIS-mediated depth imaging by confocal microscopy.**

The ability of SBIS to image cell thickness was tested in *Ectocarpus* sp. and *Saccharina latissima*. **(A, B)** Confocal microscopy. Section resulting of orthoslices in the X-Y plane is outlined in magenta, and in the Y-Z plane in yellow. The orthoslice seen at **(A)** the junction

of two cells of an *Ectocarpus* filament and **(B)** through a cellular monolayered lamina of *Saccharina*, shows that SBIS (in orange) allowed the imaging of the whole cell thickness (in z: 7 µm in *Ectocarpus,* 20 µm in *Saccharina*), in contrast to CFW (blue in B: only 5 µm of the 20 µm thick cell was labeled). Orthoslice made with (A) ZEN Blue 3.9 software and (B) Imaris 10.2.0 software. **(C)** 3D reconstruction of a confocal z-stack of a region of the *Saccharina* lamina labeled with SBIS (in orange). Chloroplasts (CP in red) are scattered within the cell volume (middle panel) and cell shape is clearly outlined (right panel: cell shape 1 and cell shape 2 schematically drawn in white). 3D reconstruction done using Imaris 10.2.0 software. **(D)** When using the Airyscan mode of the confocal microscope, SBIS-labeled *Ectocarpus* showed a sharper rendition of the boundaries of the cross wall, in contrast to CFW. However, the Airyscan mode used the 561 nm laser to excite SBIS, which also excites the chloroplasts in *Ectocarpus* cells. As a result, the image shows signals recovered from both SBIS and the chloroplasts (red *). The lower panels are enlargements of the upper panels. CFW is excited with a 405 nm laser and the detection band is 410–470 nm (Exc 405/Em 410–470). SBIS: Exc 561/Em 578–632; chloroplasts auto-fluorescence: Exc 561/Em 674–721. Scale bars represent 5 and 10 µm in A), 20 µm in B), 20 µm in C) and 5 and 10 µm in D).

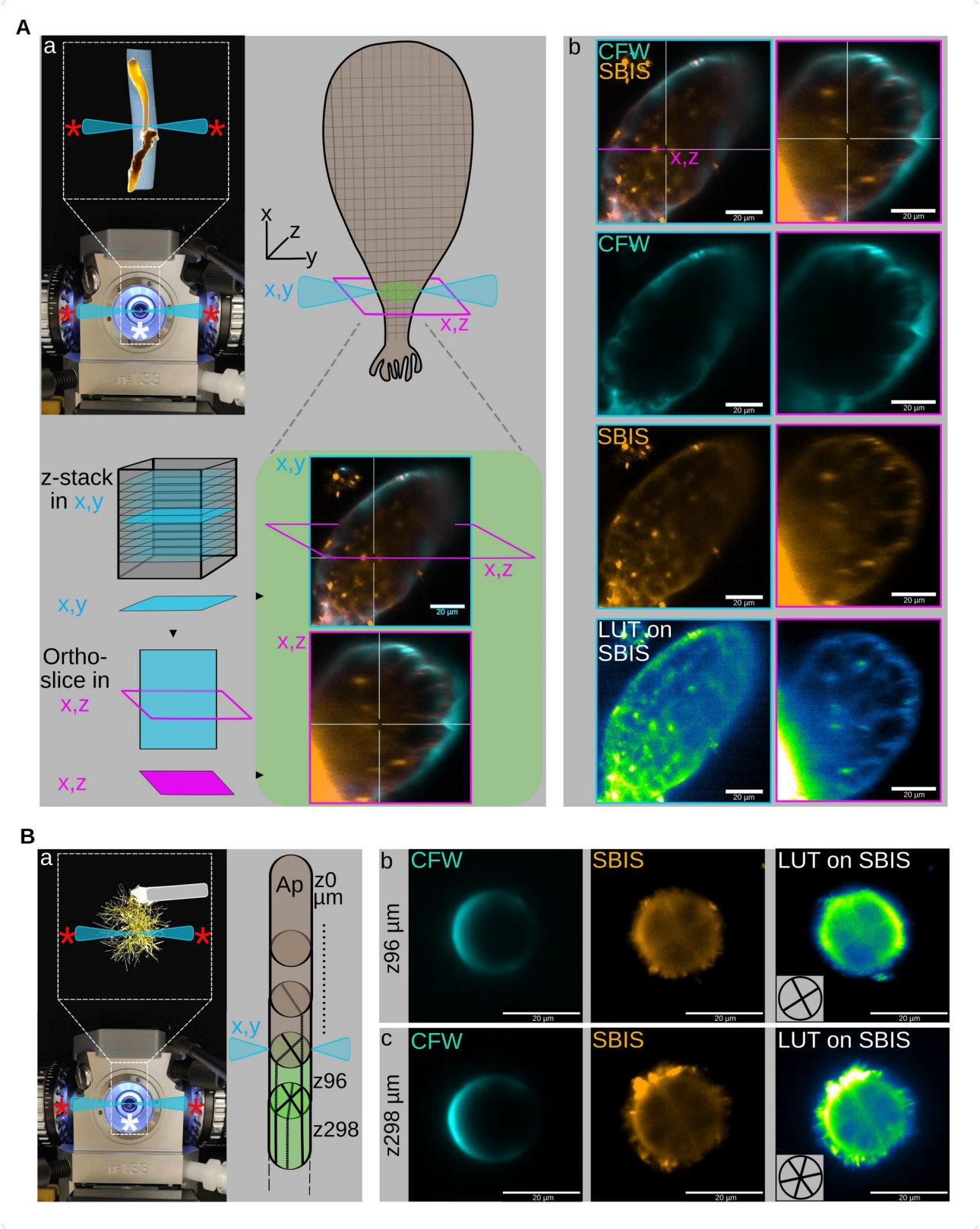

Figure 5: SBIS-mediated depth imaging in light-sheet microscopy.

The ability of SBIS to image cell thickness was tested in the brown algae *Saccharina latissima* and *Sphacelaria rigidula*. **(A)** Imaging of *Saccharina* cells in 3D using light-sheet microscopy. **(a)** Mounting of *Saccharina* in agarose between two illumination objectives (red *, light sheets schematized in blue) and in front of an observation objective (white *). Schematics of *Saccharina latissima* with the two light sheets (schematized as blue

triangles) placed to image the transition zone (TZ, green circle). Orthoslice in X/Z (in magenta) was performed at the middle of the TZ (photo below shows the Calcofluor White (CFW) signal in cyan corresponding to X/Y slice cut in the middle of the thickness (Z-axis) of the tissue and SBIS signal in orange corresponding to an X/Z section). **(b)** Top: TZ labeled with CFW (cyan) and SBIS (orange) parallel to the light sheets (z-stack; boxed in cyan) and perpendicular to it (orthoslice in X/Z boxed in magenta). Middle: Only CFW in the two orientations. Bottom: Only SBIS shown in the two orientations. CFW does not enable proper imaging of cell thickness in the TZ, whereas SBIS can distinguish cell shape throughout its thickness. **(B)** Imaging of *Sphacelaria* cells in 3D using light-sheet microscopy. **(a)** Mounting of *Sphacelaria* glued on a glass capillary to localize a filament between the two illumination objectives (red *, light sheets schematized in cyan) and in front of an observation objective (white *). Schematics of a *Sphacelaria* filament, cells below the apex (Ap) located at z0 µm develop progressively in 3D (in green). Hence, the light sheets (cyan triangles) are placed paralleled to the filament to image these cells in third axis (Z 96 µm and Z 298 µm). **(b)** Unlike CFW (cyan), SBIS (orange) labels the transverse PM of the first *Sphacelaria* cell developing in 3D located in z 96 µm, and **(c)** in z298. A Green Fire Blue LUT inferred from Fiji on the SBIS channel can help distinguish the PM. The inferred position of the new transverse PMs is displayed in the insert in the bottom left-hand corner. CFW was excited with a 405 nm laser and the detection wavelength is 415 nm (Exc 405/Em 415). SBIS: Exc 561/Em 571 nm; chloroplasts: Exc 561/Em 571 nm. Scale bars represent 20 µm in A) and B).